Estimation of Solar Radiation Energy in the Paraw Mountain of Kermanshah Province as a Rugged Topography

Somayeh Naserpour[a], Hasan Zolfaghari[a*], Parviz Zeaiean Firouzabadi[b]

[a] *Department of Geography, Razi University, P. O. Box: 67144-14971, Kermanshah, Kermanshah, Iran.*
[b] *Department of Remote Sensing and GIS, Faculty of Geographical Sciences, University of Kharazmi, P. O. Box: 15719-14911, Tehran, Tehran, Iran.*

A B S T R A C T

One of the most important characteristics of site selection for solar energy system installations and optimum solar energy harvesting in the hilly or mountainous terrains is knowledge about the amount and duration of solar radiation within such topographic terrains. Solar radiation data are not readily available for most mountain terrains because of their rugged topography. For these areas, solar radiation data can be obtained through alternative methods such as the Hemispherical Viewshed Algorithm in which spatial and temporal variations of radiation are calculated in terms of elevation, slope, and terrain. In this study, this algorithm was used to estimate and model solar radiation in the Paraw Mountain in Kermanshah. The inputs for this method were ASTER Digital Elevation Model (DEM) with a spatial resolution of 30 m and meteorological parameters that affect solar radiation. The slope and aspect maps were created from ASTER DEM and layers for monthly direct, diffuse, global, and radiation periods were generated for the year 2016. The results showed that in the Paraw Mountain, the amount of solar radiation received was dependent on the slope orientation, as the north and northeast-facing slopes received the lowest and the south and southwest-facing slopes and the flat areas received the highest direct and global radiation (i.e., in terms of this factor, these landscapes can be recommended as the best site for solar energy system installations and optimum solar energy harvesting). The sum annual radiation period varies from 382.67 to 4310.9 hours, the total radiation received annually varies between 1005.56 and 7467.3 MJ/m^2, and the sum monthly solar radiation is the highest in July (181.49-842.26 MJ/m^2) and lowest in December (25.42-319.90 MJ/m^2). Statistical error comparisons between station-based measurements and model-based estimates were performed via R^2, measures. As a result, this model was recommended for solar radiation estimation with acceptable accuracy, especially in high areas with rugged topography where solar radiation data are not readily available.

1. INTRODUCTION

The sun is the main source of life and energy on earth and biological organisms cannot survive without its light and thermal energy. Solar energy is a renewable and clean energy source and environmental phenomena have been and are exposed to its benefit for a long time. The earth receives only about one-millionth of the sun's energy and the rest of this energy mostly scatters into the solar system and beyond. The sun's surface temperature is about 6,000 °C and this temperature rises toward its inner core. The inner core of the sun is estimated to have a temperature of about 20 million degrees Celsius. On average, the sun releases about 2×10^{27} calories of thermal energy into space every minute, of which the earth receives about 2×10^{18} calories. Given the current volume of the sun, which is 2×10^{33} grams, it can maintain its current state for millions of years [1].

The installation of solar power systems in mountainous terrains should be done according to the temporal and spatial distribution of solar radiation. This distribution of energy received from the sun is to some extent dependent on astronomical, geographical, geometric, physical, and meteorological factors. Knowing the variations of solar radiation received on surfaces with different slopes and orientations is the basic requirement in several fields of industry and science, including meteorology, agriculture, photobiology, animal husbandry, lighting, architecture, and solar energy generation. In general, meteorological stations only measure the diffuse and global radiation received on the horizontal surface. Therefore, the solar radiation data for sloping surfaces are not readily available and must be calculated based on the values given for horizontal surfaces [2]. The intensity of solar radiation received on the surface is determined by three factors: 1- solar incidence angle, which depends on the slope and season, 2- cloudiness and pollution, which depend on the region's climate and meteorological conditions, and 3- topography, which depends on elevation, ground slope angle and aspect, and dominant gradient of the area. Elevation, zenith angle, and horizontal barriers to radiation (due to adjacent topography) can significantly impact the amount of radiation reaching the ground surface

*Corresponding Author's Email: h.zolfaghari@razi.ac.ir (H. Zolfaghari)
URL: http://www.jree.ir/article_122116.html

[3]. Total solar radiation received on a sloping surface consists of three components: direct solar radiation, diffuse solar radiation (solar radiation arriving indirectly on the surface after having been scattered in the atmosphere), and reflected solar radiation (reflected from the earth's surface). Some researchers have used empirical models (Including Liu and Jordan [4], Hay [5], Steven and Unsworth [6], Reindl et al. [7], and Tian et al. [8]). In addition to these models, this estimation can be carried out using the Solar Analyst as an ArcView GIS extension, which allows researchers to compute total radiation and its components including direct, diffuse, and reflected radiation for different topographies. Topography has a great impact on the received solar radiation, particularly because the angle and aspect of ground slopes can be such that the site receives reduced direct sunlight. Changes in the angle and aspect of slopes can determine the radiation angle and the amount of thermal energy received in different landscapes [9]. The solar radiation analysis tool is the spatial analysis program that can estimate, analyze, and visualize this parameter in any part of the globe at any time. Using this tool, one can determine the effects of atmospheric conditions, longitude and latitude, altitude, angle, and aspect of slopes, daily and seasonal changes in solar angles, and shading of heights on the amount of solar radiation that reaches the earth's surface. Therefore, this tool can be used to facilitate analyses in many studies that involve solar radiation calculations [10]. For instance, Hofierka and Suri [11] developed a flexible GIS-based model called r.sun for solar radiation modeling, which is fully integrated into the open-source GIS environment. This model can calculate all solar radiation components (e.g., direct, diffuse, and reflected radiation) for clear and cloudy skies and is especially suitable for modeling large areas with complex terrains. This model can be easily used in long-term solar radiation calculations on different scales and also in the estimation of temporal variations of solar radiation (over a day or a year). Dozier and Frew [12] proposed rapid algorithms by which the Digital Elevation Model (DEM) can be used for quick calculation of terrain parameters to estimate the incoming solar and longwave radiation in surface climate models so as to reduce the computation times of these models. In another study, Geographic Information System (GIS) was used to estimate the solar energy potential in Karnataka state, India and identify suitable areas for using solar energy. This study found that the coastal parts of Karnataka were more suitable for using solar energy [13]. Pons and Ninyerola [14] also proposed a GIS-based model for the estimation of solar radiation based on astronomical, atmospheric, and geographic factors with DEM used as input. In another study, Battles et al. [15] used the radiation analysis tool of the ArcGIS software to estimate the amount of solar radiation in areas with complex topography. The results of this study showed that the software provided a more accurate estimate of solar radiation in the summer months than in the winter months. Other researchers have also used this tool to estimate solar radiation potential in their areas of interest. These include Gastli and Charabi [16] who used this tool to determine the potential for harvesting solar energy in Oman. The results of this study showed that this region had a very high solar radiation potential throughout the year. This study estimated that implementing CSP technology in only 10 percent of Oman's flat terrain (land with a slope of less than 1 percent) would result in the annual generation of 7.6 million gigawatts

of electricity, which is 680 times more than the existing electricity generation capacity of this country (in 2007, this capacity was about 11,189 (GWh)). In the end, these researchers produced an annual solar radiation map for the studied area. Several studies have used the Solar Analyst to evaluate the potential of harvesting solar energy and identify suitable areas for the installation of solar systems. For example, this approach was used in a study in Hong Kong to estimate the region's solar energy potential and identify suitable areas for solar panels. This study claimed that its methods and findings provided an accurate estimate of solar energy potential throughout Hong Kong, thereby facilitating renewable energy production in this area [17]. Also, radiation modeling using GIS-based models was carried out by Zhang et al. [18] for the Qilian Mountains, Northwest China, Zhang et al. [19] for Northwest China, and Moren et al. [20] for the upper Green River basin in Wyoming, U.S. The GIS-based solar radiation models can provide spatial data, planning, and design of solar energy systems, preparing radiation maps of specific areas for different periods and estimating the potential of the point or area [21]. Potential solar radiation modeling, site selection for solar energy systems installations, and thus electricity generation allow one to generate different scenarios for future sustainable planning powered by smart distribution grids with integrated energy storage [22]. PV systems are used for different purposes [23, 24, 25]. The number of solar lighting systems in the top five countries, to End-2014, is given below: solar lighting systems in India (960,000), Tanzania (790,038), Kenya (764,900), Ethiopia (661,630), and Uganda (84,352). The number of solar home systems in top five countries to end-2014 is as follows: solar home systems in Bangladesh (3,600,000), India (1,100,000), China (500,000), Nepal (500,000), and Kenya (320,000) [26]. Installing these systems is very suitable for meeting the electrical needs of areas without a national electricity grid (including rugged terrains). Many rural areas of Iran are situated on mountainous terrains with rugged topography. One of the main problems of highly remote rural areas is the lack of access to electricity, as it is difficult and expensive to construct and maintain long transmission lines over rugged terrains. The most appropriate solution for supplying electricity in these areas is the use of solar energy technology. Therefore, the electricity of off-grid photovoltaic systems is technically and economically convenient for these rural settlements than connecting them to the national grid. Therefore, for appropriate utilization of solar radiation energy in these mountain villages, modeling of spatial and temporal variations of radiation and site selection (due to topographic characteristics) for installing the photovoltaic (PV) is critically important. Solar radiation data are not available for many of these areas. These data need to be obtained using alternative methods. In the present study, the Solar Analyst (as an ArcView GIS extension) was used to model the solar radiation condition and its components in the Paraw Mountain (Kermanshah, Iran), which has a complex topography, to estimate the solar radiation received in this mountain and its temporal-spatial variations and also evaluate the performance of this approach in estimating radiation in complex topographies and sloping terrains. Applying this method can help evaluate the solar radiation condition and its components in mountainous terrain and suggest the best site for installing solar energy systems in mountain villages, mountain shelters, nomadic tents, and mountain roads.

2. MATERIALS AND METHODS

2.1. Study area and data

This study was focused on the solar radiation condition and its components in the Paraw Mountain in Kermanshah, Iran. The geographical location of the Paraw Mountain is shown in Figure 1 (34^0 25′ 05 N latitude 47^0 14′ 34 E longitude). This mountain stretches from the northwest to the northeast of the city of Kermanshah and is part of the Zagros mountain range in western Iran. The highest peak of this mountain is the Paraw peak in the northeast of Kermanshah, which has a height of 3386 meters above sea level. However, this mountain has two other peaks called Bisotun and Taq-e Bostan, which are more widely known because of their historical significance. The daily solar radiation measurements made at Kermanshah Meteorological Station in 2016 were collected from Iran Meteorological Organization [27]. These measurements were subjected to a quality control process before they could be used in analyses. The digital elevation model of the study area was extracted from the DEM derived from the Advanced Spaceborne Thermal Emission and Reflection Radiometer (ASTER) with a spatial resolution of 30 meters, which were downloaded from the USGS earth explorer website [28].
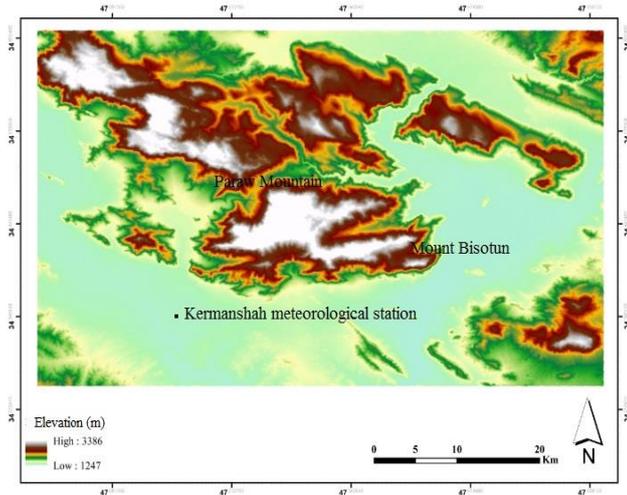

Figure 1. Digital elevation model of the study area (Paraw Mountain and Kermanshah synoptic station)

2.2. METHOD

2.2.1. The solar analyst tools in Arc Map

One way to estimate the amount of radiation received in complex terrains is to use the Solar Analyst tools in Arc Map. This tool operates based on methods from the hemispherical viewshed algorithm and performs calculations through four steps:

1. The calculation of an upward-looking hemispherical viewshed based on topography.
2. Overlay of the viewshed on a direct sun map to estimate direct radiation.
3. Overlay of the viewshed on a diffuse sky map to estimate diffuse radiation.
4. Repeating the process for every location of interest to produce an insolation map [29].

This algorithm is used to calculate the solar radiation for each site and produce an accurate radiation map, and its inputs

for calculating solar radiation are elevation, latitude, slope angle, slope aspect, and the angle of incidence, all of which affect the incoming radiation. Using this tool, one can estimate the total solar radiation and its components, including direct, diffuse, and reflected radiation for different topographies.

2.2.2. Global solar radiation calculation

The sum of direct and diffuse radiation that reaches the earth's surface in a unit of time (minute, day, month, and year) is called global radiation. Therefore, global radiation on a given surface can be obtained by summing the direct and diffuse shortwave radiations [30]. The analyses of this step were implemented using the following equations given by Rich et al. [31]; Rich and Fu [32]; Fu [33]; Fu and Rich [34]; Fu and Rich [35]:

Global solar radiation or Global$_{sum}$ is calculated as the sum of direct radiation (Dir$_{sum}$) and diffuse radiation (Dif$_{sum}$) of all sun map and sky map sectors, respectively.

$$Global_{sum} = Dir_{sum} + Dif_{sum}$$

2.2.3. Direct solar radiation calculation

The sum of direct radiation (Dir$_{sum}$) for a given site is the sum of the direct incoming solar radiation (Dir$_{\theta,\alpha}$) from all sun map sectors Eq. (1). The direct solar radiation from the sun map sector (Dir$_{\theta,\alpha}$) with a centroid at zenith angle (θ) and azimuth angle (α) is calculated using Eqs. (2-3). The angle of incidence (AngInSky$_{\theta,\alpha}$) is calculated using Eq. (4). Equations (1) to (4) are shown in Table 1.

Table 1. The equations of direct solar radiation calculation

Direct solar radiation calculation	Equations No.
$Dir_{sum} = \Sigma\ Dir_{\theta,\alpha}$	(1)
$Dir_{\theta,\alpha} = S_{Const} * \beta^{m(\theta)} * SunDur_{\theta,\alpha} *$ $SunGap_{\theta,\alpha} * cos(AngIn_{\theta,\alpha})$	(2)
$m(\theta) = EXP(-0.000118 * Elev -$ $1.638*10^{-9} * Elev^2) / cos(\theta)$	(3)
$AngIn_{\theta,\alpha} = acos(\ Cos(\theta) * Cos(G_z) +$ $Sin(\theta) * Sin(G_z) * Cos(\alpha - G_a)\ )$	(4)

2.2.4. Diffuse solar radiation calculation

The sum of diffuse radiation was calculated by the gap fraction and angle of incidence using Eqs. (5-6) and for the uniform sky diffuse model, Weight$_{\theta,\alpha}$ was calculated by Eq. (7). For the standard overcast sky model, Weight$_{\theta,\alpha}$ was calculated by Eq. (8). The sum of diffuse radiation for the location (Dif$_{sum}$) was calculated as the sum of the diffuse solar radiation (Dif) from all the sky map sectors using Eq. (9). Equations (5) to (9) are shown in Table 2.

Table 2. The equations of diffuse solar radiation calculation

Diffuse solar radiation calculation	Equations No.
$Dif_{\theta,\alpha} = R_{glb} * P_{dif} * Dur * SkyGap_{\theta,\alpha} *$ $Weight_{\theta,\alpha} * cos(AngIn_{\theta,\alpha})$	(5)
$R_{glb} = (S_{Const}\ \Sigma(\beta^{m(\theta)})) / (1 - P_{dif})$	(6)
$Weight_{\theta,\alpha} = (cos\theta_2 - cos\theta_1) / Div_{azi}$	(7)
$Weight_{\theta,\alpha} = (2cos\theta_2 + cos2\theta_2 - 2cos\theta_1 -$ $cos2\theta_1) / 4 * Div_{azi}$	(8)
$Dif_{sum} = \Sigma\ Dif_{\theta,\alpha}$	(9)

2.2.5. Error evaluation test

To validate results, the available data were used to compute daily global solar radiation for the first days of each month, solstices, and equinoxes. Then, the results were compared with the total solar radiation measurements made at Kermanshah meteorological station. This comparison was made using the coefficient of determination (R^2) statistic, which is defined as follows [36, 37, 38]:

$$R^2 = \frac{\sum_{i=1}^{N}(G_i-G_m)^2}{\sum_{i=1}^{N}(G_i-\overline{G_m})^2} \tag{10}$$

where n is the number of observations, G_i is the estimated daily global solar radiation, G_m is the measured daily global solar radiation, and $\overline{G_m}$ is the mean of daily global solar radiation measurements. The closer the R^2 value is to 1, the better the model performance will be.

3. RESULTS AND DISCUSSION

This section presents the results of solar radiation calculations implemented based on Equations 1 to 9. The duration or daylength, which is controlled by the rotation of the earth around its axis [39]. The longer the radiation duration is, the greater is the sum amount of solar radiation energy reaching the surface [30]. Calculations related to the duration in the study area are shown in Figure A1 (see Fig. A1 in Appendix). As shown in this figure, the monthly total radiation duration for January varies from 0 to 284.90 hours. The figure is 0-300.18 for February, 0-352.72 for March, 1.01-374.02 for April, 92.90-409.75 for May, 91.27-412 for June, 101.97-418.74 for July, 20.45-396.91 for August, 0-350.13 for September, 0-327.09 for October, 0-288.36 for November, and 0-236.52 hours for December. The highest monthly sum radiation durations are for May, June, and July (with very close values) and the lowest is for December. Comparing the radiation duration maps of the study area with the slope aspect map (Figure 2) shows that the south (with aspect between 157.5–202.5) and southwest-facing slopes (with aspect between 202.5–247.5) and the flat areas have the longest radiation durations and the north and northeast-facing slopes have the lowest radiation durations.
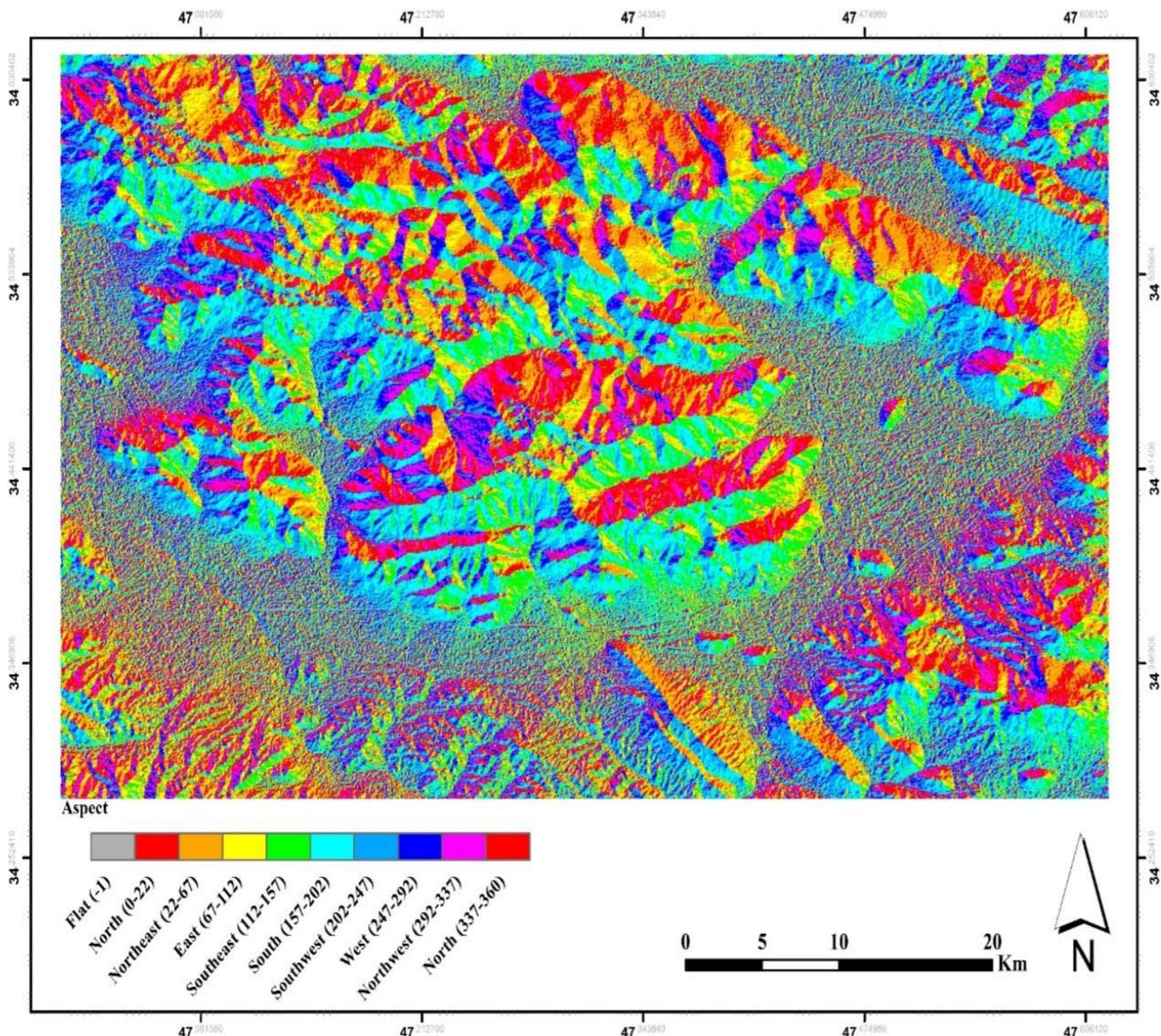

Figure 2. Map of aspect in the study area

The estimations made for direct, diffuse, and global solar radiations in the study area are provided in Table 3. As this table shows, the total direct radiation is the highest in July and the lowest in December (from 100,935 to 655.1568 MJ/m^2 for July and from 0 to 255.9125 MJ/m^2 for December). Comparing the total direct radiation maps with the aspect map as one of the important criteria for installing PV systems (Figure 2) shows that the south, southwest, and west-facing slopes and the flat areas (plains) receive the highest amount of direct radiation and the north, northeast and to some extent, northwest-facing slopes receive the lowest direct radiation. The maps of direct solar radiation estimates for the study area are shown in Figure A2 (see Fig. A2 in Appendix). The share of diffuse solar radiation in the total monthly radiation is the highest in July and the lowest in December. The diffuse solar radiation estimates obtained for the area vary from 68.4104 to 187.1345 MJ/m^2 for July and from 25.4205 to 77.2614 MJ/m^2 for December. However, comparing the diffuse solar radiation maps with the aspect map shows that the diffuse radiation has not the same distribution in the area as direct and global radiation, because the north and northeast-facing slopes receive the highest amounts of diffuse radiation, and the south and southwest-facing slopes and the flat areas have the lowest amounts of diffuse radiation. The maps of diffuse solar radiation estimates for the study area are shown in Figure A3.

The estimations of global solar radiation in the study area indicate that as in the above cases, July has the highest and December has the lowest monthly global radiation. For July, this estimate ranges from 181, 4857 to 842, 2632 MJ/m^2, and for December, it varies from 25, 4205 to 319,901 MJ/m^2. Comparing the monthly global radiation maps with the aspect map shows that the global radiation is the lowest in the north and northeast-facing slopes and the highest in the south and southwest-facing slopes and the flat areas. The maps of global radiation estimates for the study area are presented in Figure A4 (see Fig. A4 in Appendix).

Comparing the radiation received in flat areas with the radiation received in sloped areas, especially at higher elevations, shows that the amount of radiation received increases with altitude. At higher altitudes, thickness of the atmosphere is lower and thinner because air molecules can spread out more and air density decreases. Therefore, these areas have the highest potential for receiving solar radiation [40]. According to the maps of total annual radiation duration in the study area (2016), this parameter ranges from a minimum of 382.674 hours to a maximum of 4310.9 hours. The minimum and maximum diffuse radiations, direct radiation, and global radiation received annually are 606.4596 and 1702.984 MJ/m^2, 336.8423, and 5840.674 MJ/m^2, and 1005.556 and 7467.3 MJ/m^2 (per year), respectively.

Table 3. The sum of, direct, diffuse, global and duration radiations estimated at Kermanshah station by The Solar Analyst in 12 months

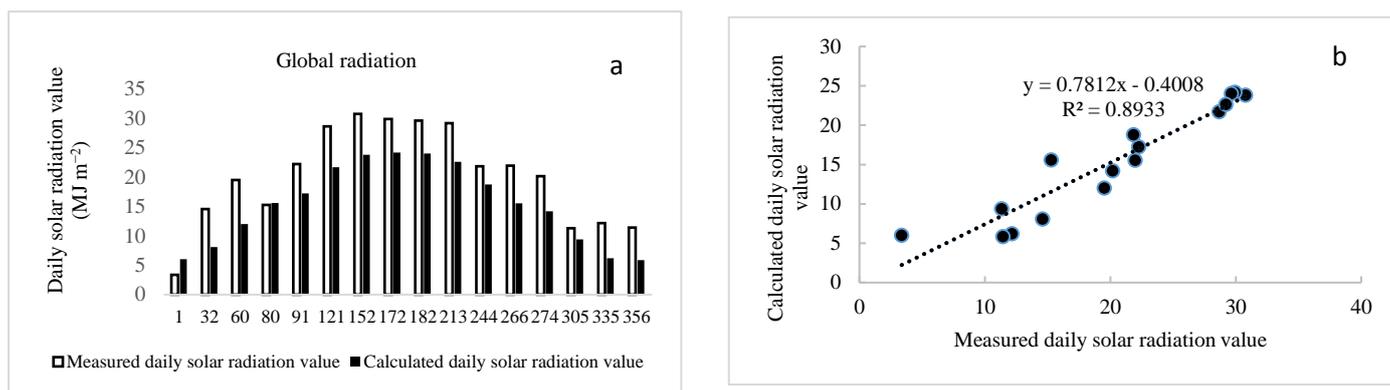| Month	Maximum diffuse radiation (MJ m^{-2})	Minimum diffuse radiation (MJ m^{-2})	Maximum direct radiation (MJ m^{-2})	Minimum direct radiation (MJ m^{-2})	Maximum global radiation (MJ m^{-2})	Minimum global radiation (MJ m^{-2})
Jan.	84.09	28.03	337.08	0.00	406.76	28.03
Feb.	103.20	35.63	402.91	0.00	488.51	35.63
Mar.	139.87	49.78	515.92	0.00	642.82	51.21
Apr.	160.62	58.21	571.50	0.65	725.13	63.00
May	183.71	67.09	649.05	74.97	831.41	148.98
Jun.	184.49	67.51	644.43	125.70	828.89	211.94
Jul.	187.13	68.41	655.16	100.94	842.26	181.49
Aug.	172.31	62.64	608.68	13.30	777.01	80.33
Sep.	143.34	51.36	521.46	0.00	654.11	53.87
Oct.	118.75	41.40	451.64	0.00	553.67	41.40
Nov.	89.13	29.98	353.14	0.00	427.01	29.98
Dec.	77.26	25.42	255.91	0.00	319.90	25.42
Annual total	1702.98	606.46	5840.68	336.84	7467.30	1005.56

Figure 3. Comparison of measured daily global solar radiation and calculated daily global solar radiation by Solar Analyst (a) and its determination coefficient (b)

To measure the accuracy and performance of the Solar Analyst, the method was used to estimate the global solar radiation in Kermanshah meteorological station for the first day of each month and solstices and equinoxes, and the results were compared with the measured data. The coefficient of determination (R^2) was then computed so that the accuracy of the software in estimating radiation could be evaluated. According to Figure 3, this model was recommended for solar radiation estimation with acceptable accuracy, especially in high areas with complex topography where solar radiation data are not available.

4. CONCLUSIONS

The Solar Analyst tools provided in the ArcMap software can estimate the radiation received at any given point or across an area. To assess the spatial and temporal distribution of solar radiation in the Paraw Mountain, in this study, this tool was used to estimate the direct, diffuse, and global solar radiation and the duration of radiation in this area for different months of 2016. The estimations of radiation duration showed that in this area, May, June, and July experienced the highest and December had the lowest monthly total radiation duration. The results also showed that the south and southwest-facing slopes and the flat areas had the highest radiation durations and the north and northeast-facing slopes had the shortest radiation durations.

The estimations of direct, diffuse, and global solar radiations in the study area showed that July had the highest and December the lowest amounts of total monthly radiation. It was found that the diffuse radiation was the highest in the north and northeast-facing slopes and the lowest in the south and southwest-facing slopes and the flat areas. For both direct and global radiations, the estimates were the lowest in the north and northeast-facing slopes and the highest in the south and southwest-facing slopes and the flat areas. The results also showed that in the Paraw Mountain, the amount of radiation increased with altitude. The total annual solar radiation duration in the study area (2016) was estimated to range from a minimum of 382.674 hours to a maximum of 4310.9 hours. The total global radiation in the area was estimated to be between 1005.556 and 7467.3 MJ/m^2 per year. The standard amount of solar radiation for PV system installations is $> = 1.15$ MWh/m^2/yr or 4140 MJ/ m^2/yr [41]; as a result, this site is suitable for solar energy harvesting.

In the performance evaluation of the employed tool, the coefficient of determination (R^2) was calculated as 0.89. This evaluation showed the acceptable accuracy of the model and

that the tool could have accurate solar radiation estimates, which is subsequently used in the site location of solar panels, for areas without radiometric stations and those with high altitudes and complex terrains. This conclusion is consistent with the findings of Sabziparvar et al. (2015), who used the same tool to estimate the total radiation in four provinces of Iran, used statistical tests to compare the results with the measurements, and ultimately reported the good accuracy of this method in estimating total solar radiation. The results were also consistent with the findings of Valizadeh (2014), which showed the acceptable speed and accuracy of this tool in estimating solar radiation. The studies of Hofierka and Suri (2002), Ramachandra (2006), Pons and Ninyerola (2008), and Moren et al. (2018) reached similar conclusions.

5. ACKNOWLEDGEMENT

NOMENCLATURE

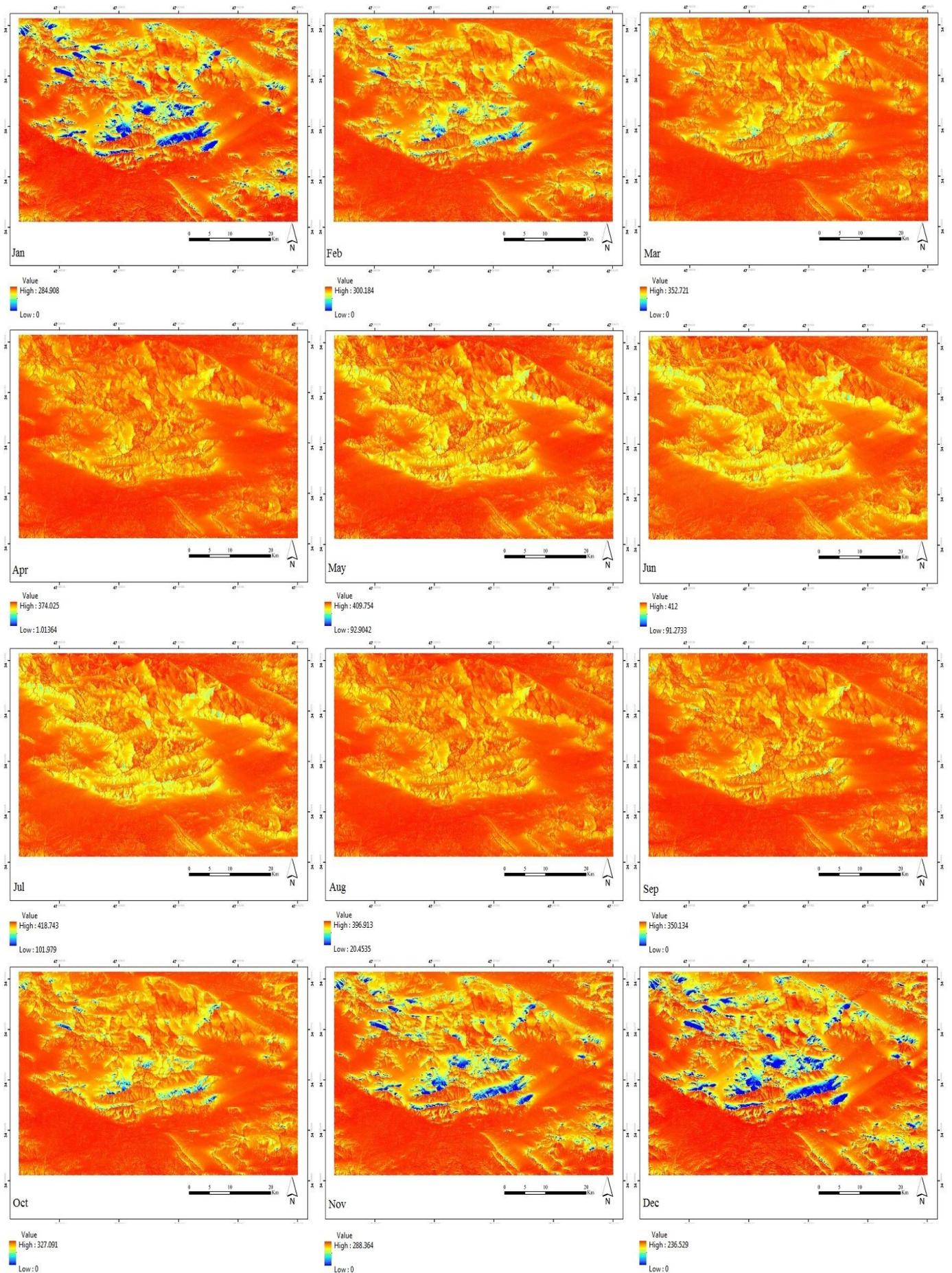|	
S_{Const}	Solar constant (1367 Wm^{-2})
β	The transmissivity of the atmosphere
$m(\theta)$	The relative optical path length
$SunGap_{\theta,\alpha}$	The gap fraction for the sun map sector
$SunDur_{\theta,\alpha}$	The time duration or potential daylength
$AngIn_{\theta,\alpha}$	The angle of incidence between the centroid of the sky sector and the axis normal to the surface
θ	The solar zenith angle
Elev	Altitude of site (m)
G_z	The surface zenith angle
G_a	The surface azimuth angle
R_{glb}	The global normal radiation
P_{dif}	The proportion of global normal radiation flux that is diffused
Dur	The time interval for analysis
$SkyGap_{\theta,\alpha}$	The gap fraction for the sky sector
$Weight_{\theta,\alpha}$	The proportion of diffuse radiation originating in a given sky sector relative to all sectors
R_{glb}	The global normal radiation
R^2	Coefficient of determination
θ_1 and θ_2	The bounding zenith angles of the sky sector
Div_{azi}	The number of azimuthal divisions in the sky map

Appendix

See Figs. A1–A4.

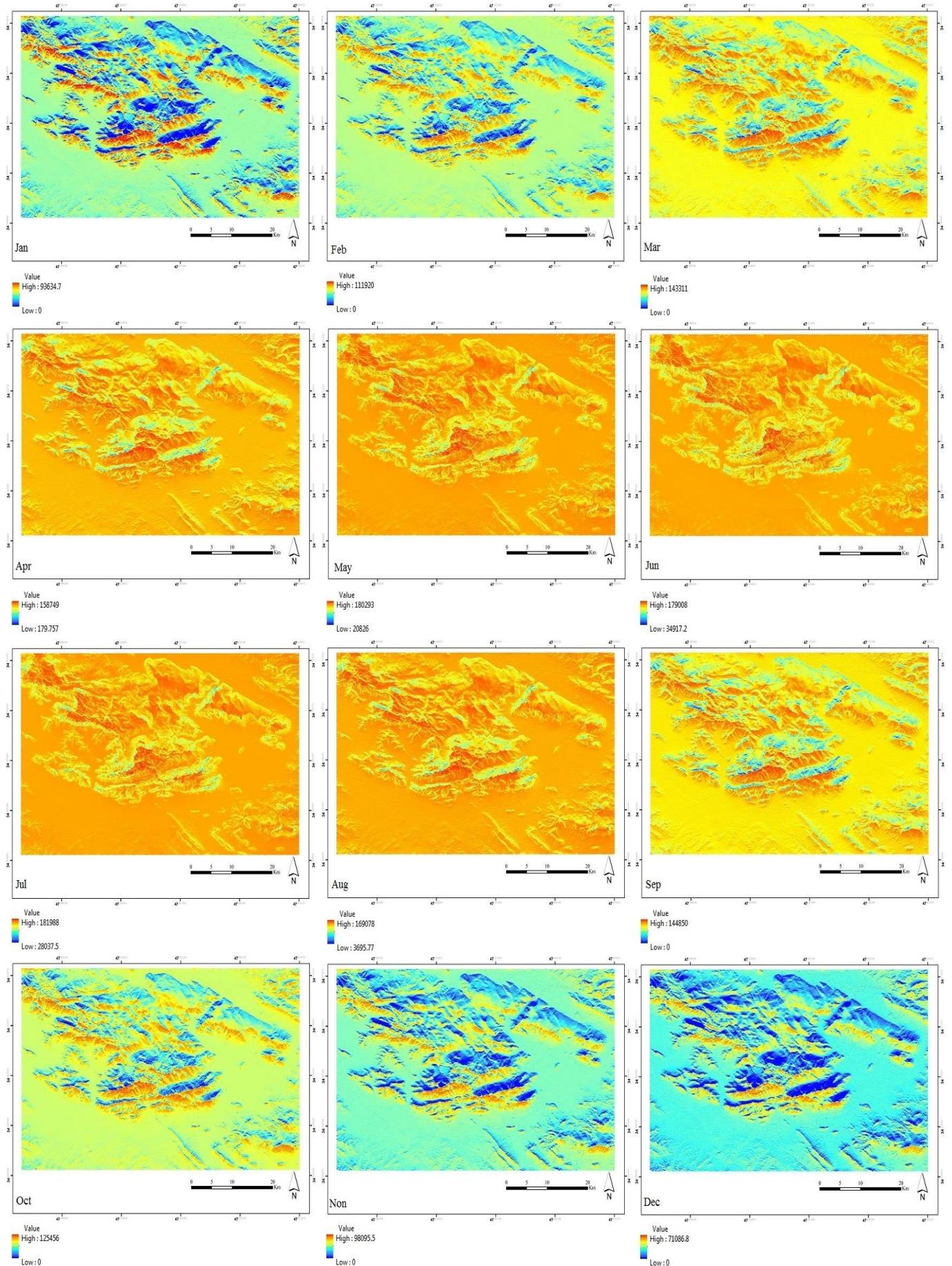**Figure A1.** Radiation duration map in the study area in 12 months of 2016

Figure A2. Temporal and spatial distribution of the sum of direct radiation in the study area in 12 months of 2016. The unit of radiation in the maps is (Wh/m^{-2})
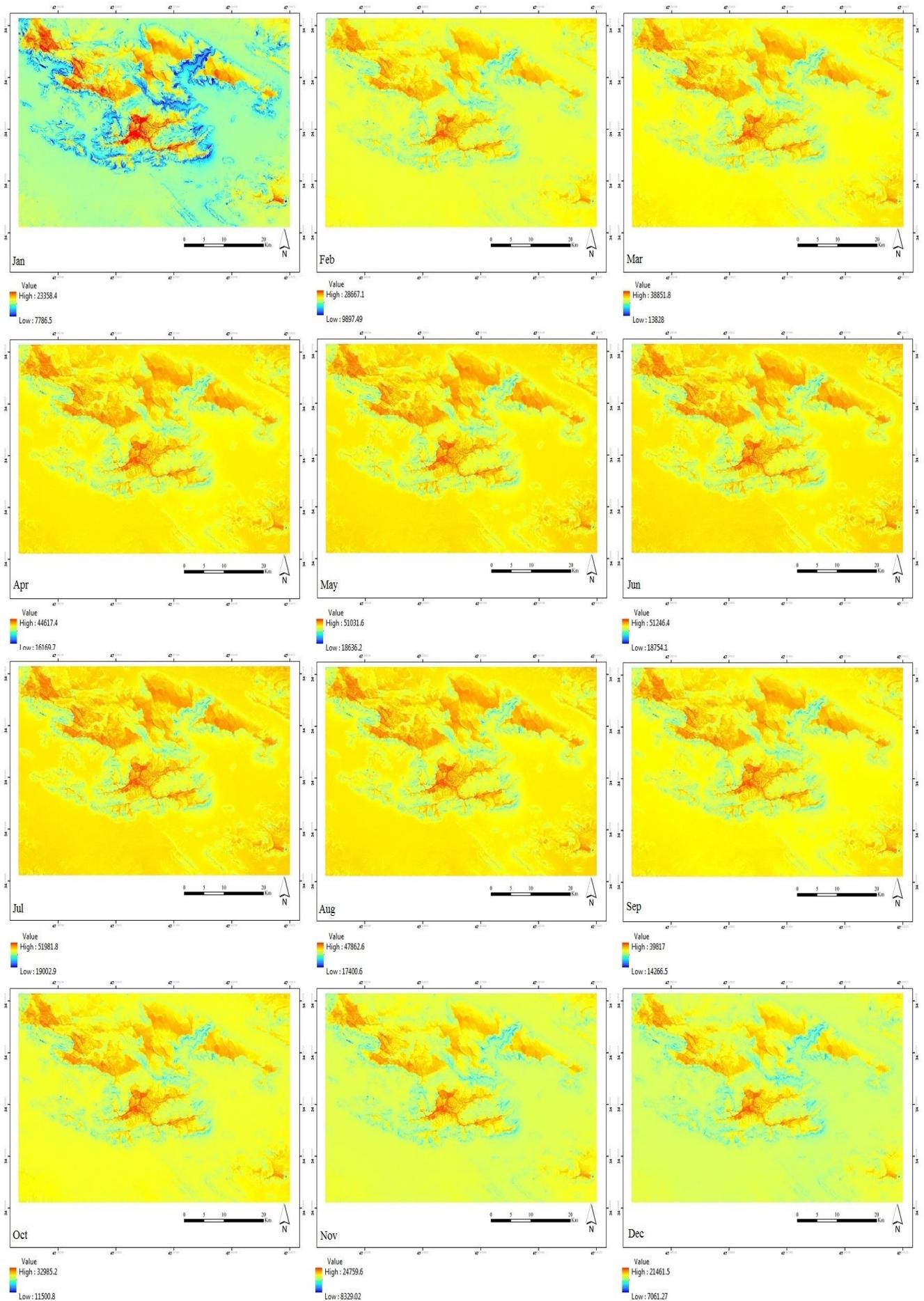
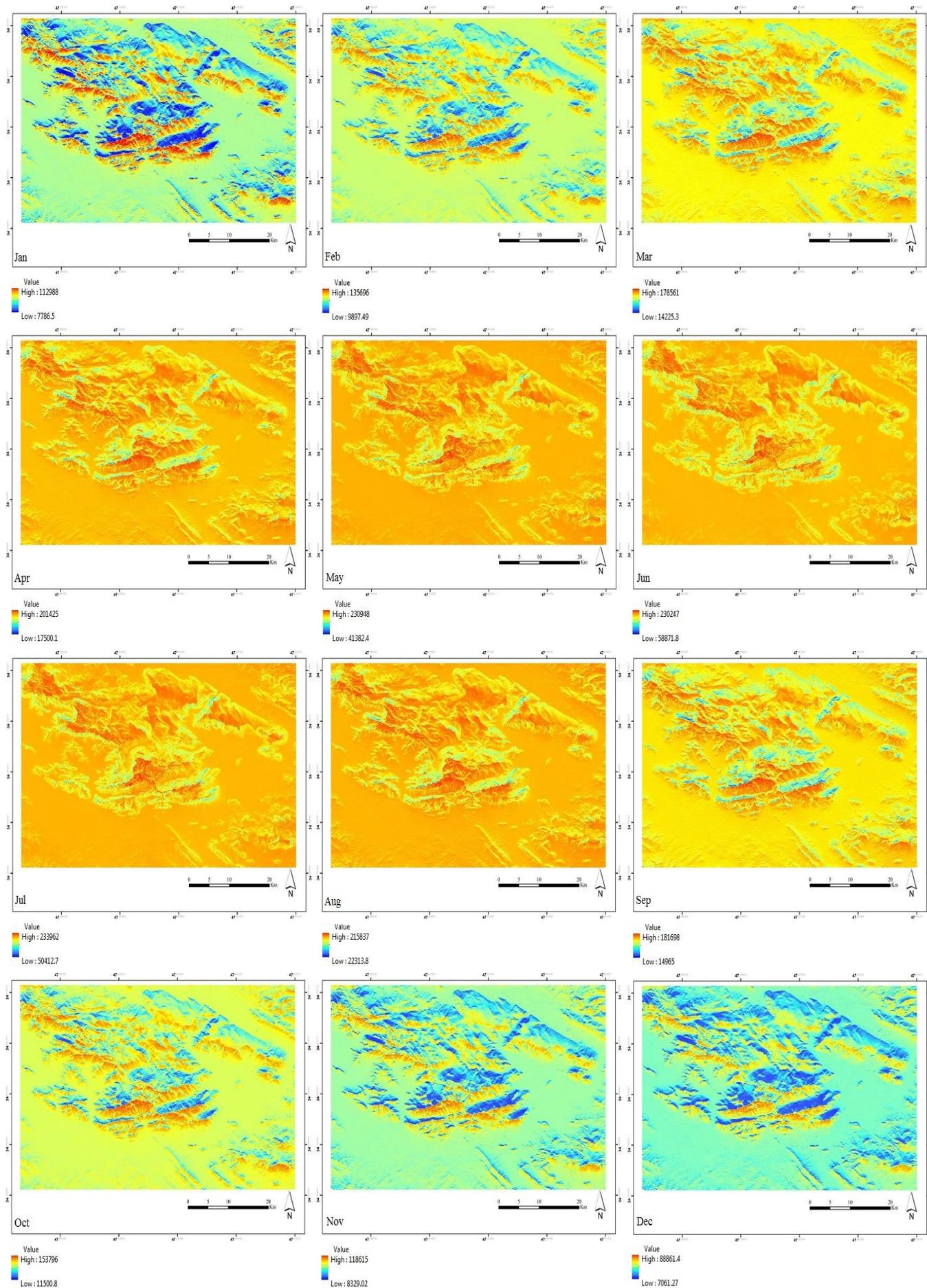**Figure A3.** Temporal and spatial distribution of the sum of diffuse radiation in the study area in 12 months of 2016

Figure A4. Temporal and spatial distribution of the sum of global radiation in the study area in 12 months of 2016

REFERENCES

1. Mostaufiolmamaleki, R., Essentials of astronomy Earth in the universe, Scientific Publication Center of Islamic Azad University Press, (1996). (http://www.lib.ir).

2. Tavousi, T., The climatic application of solar radiation in environmental planning, Sistan and Baluchestan University Press, Zahedan, (2017). (https://climatology.ir/wp-content/uploads/2017/11/Solar-Radiation.pdf).

3. Sabziparvar, A., Khatar, B. and Mohebzadeh, H., "Assessment of GIS ability in zonation of the seasonal and annual distribution of total solar radiation (Case study: Central provinces of Iran)", *Iranian Journal of Geophysics*, Vol. 9, No. 2, (2015), 14-29. (In Farsi). (http://www.ijgeophysics.ir/article_33580.html).

4. Liu, B. and Jordan, R., "Daily insolation on surfaces tilted towards equator", *ASHRAE Journal*, Vol. 10, (United States), (1961). (https://www.osti.gov/biblio/5047843-daily-insolation-surfaces-tilted-towards-equator).

5. Hay, J.E., "Calculation of monthly mean solar radiation for horizontal and inclined surfaces", *Solar Energy*, Vol. 23, No. 4, (1979), 301-307. (https://doi.org/10.1016/0038-092X (79)90123-3).

6. Steven, M.D. and Unsworth, M.H., "The angular distribution and interception of diffuse solar radiation below overcast skies", *Quarterly Journal of the Royal Meteorological Society*, Vol. 106, No. 447, (1980), 57-61. (https://doi.org/10.1002/qj.49710644705).

7. Reindl, D.T., Beckman, W.A. and Duffie, J.A., "Evaluation of hourly tilted surface radiation models", *Solar Energy*, Vol. 45, No. 1, (1990), 9-17. (https://doi.org/10.1016/0038-092X (90)90061-G).

8. Tian, Y.Q., Davies-Colley, R.J., Gong, P. and Thorrold, B.W., "Estimating solar radiation on slopes of arbitrary aspect", *Agricultural and Forest Meteorology*, Vol. 109, No. 1, (2001), 67-74. (https://doi.org/10.1016/S0168-1923 (01)00245-3).

9. Kavyani, M.R. Microclimatology, Tehran: Samt Press, (2012). (https://samta.samt.ac.ir/content/13634/%D9%85%DB%8C%DA%A9% D8%B1%D9%88%DA%A9%D9%84%DB%8C%D9%85%D8%A7%D 8%AA%D9%88%D9%84%D9%88%DA%98%DB%8C?lang=en).

10. Valizadeh Kamran, K. "Estimation of potential evapotranspiration with Estefnz method and GIS techniques in Eastern Azerbaijan", *Journal of Geography and Planning*, Vol. 18, No. 49, (2014), 317-334. (In Farsi). (https://geoplanning.tabrizu.ac.ir/article_2217.html).

11. Hofierka, J. and Suri, M., "The solar radiation model for open source GIS: Implementation and applications", *Proceedings of The Open Source GIS-GRASS User's Conference*, Vol. 2002, (2002), 51-70. (https://www.scirp.org/(S(351jmbntvnsjt1aadkposzje))/reference/Refere ncesPapers.aspx?ReferenceID=1413518).

12. Dozier, J. and Frew, J., "Rapid calculation of terrain parameters for radiation modeling from digital elevation data", *IEEE Transactions on Geoscience and Remote Sensing*, Vol. 28, No. 5, (1990), 963-969. (https://doi.org/10.1109/36.58986).

13. Ramachandra, T.V., "Solar energy potential assessment using GIS", *Energy Education Science and Technology*, Vol. 18, No. 1/2, (2006), 101. (https://www.researchgate.net/publication/256454051_Solar_energy_po tential_assessment_using_GIS).

14. Pons, X. and Ninyerola, M., "Mapping a topographic global solar radiation model implemented in a GIS and refined with ground data", *International Journal of Climatology*, Vol. 28, No. 13, 1821-1834. (https://doi.org/10.1002/joc.1676).

15. Batlles, F.J., Bosch, J.L., Tovar-Pescador, J., Martinez-Durban, M., Ortega, R. and Miralles, I., "Determination of atmospheric parameters to estimate global radiation in areas of complex topography: Generation of global irradiation map", *Energy Conversion and Management*, Vol. 49, No. 2, 336-345. (https://doi.org/10.1016/j.enconman.2007.06.012).

16. Gastli, A. and Charabi, Y., "Solar electricity prospects in Oman using GIS-based solar radiation maps", *Renewable and Sustainable Energy Reviews*, Vol. 14, No. 2, (2010), 790-797. (https://doi.org/10.1016/j.rser.2009.08.018).

17. Wong, M.S., Zhu, R., Liu, Z., Lu, L., Peng, J., Tang, Z. and Chan, W.K., "Estimation of Hong Kong's solar energy potential using GIS and remote sensing technologies", *Renewable Energy*, Vol. 99, (2016), 325-335. (https://doi.org/10.1016/j.renene.2016.07.003).

18. Zhang, Y., Chang, X. and Liang, J., "Comparison of different algorithms for calculating the shading effects of topography on solar irradiance in a

19. mountainous area", *Environmental Earth Sciences*, Vol. 76, No. 7, (2017), 295. (https://doi.org/10.1007/s12665-017-6618-5).

19. Zhang, Y.L., Li, X., Cheng, G.D., Jin, H.J., Yang, D.W., Flerchinger, G.N., Chang, X.L., Wang, X. and Liang, J., "Influences of topographic shadows on the thermal and hydrological processes in a cold region mountainous watershed in northwest China", *Journal of Advances in Modeling Earth Systems*, Vol. 10, No. 7, (2018), 1439-1457. (https://doi.org/10.1029/2017MS001264).

20. Moreno, H.A., Ogden, F.L. and Alvarez, L.V., "Unstructured-mesh terrain analysis and incident solar radiation for continuous hydrologic modeling in mountain watersheds", *Water*, Vol. 10, No. 4, (2018), 398. (https://doi.org/10.3390/w10040398).

21. Choi, Y., Suh, J. and Kim, S.M. "GIS-based solar radiation mapping, site evaluation, and potential assessment: A review", *Applied Sciences*, Vol. 9, No. 9, (2019),1960. (https://doi.org/10.3390/app9091960).

22. Buffat, R., Grassi, S. and Raubal, M., "A scalable method for estimating rooftop solar irradiation potential over large regions", *Applied Energy*, Vol. 216, (2018), 389-401. (https://doi.org/10.1016/j.apenergy.2018.02.008).

23. Hoseinzadeh, S. and Azadi, R., "Simulation and optimization of a solar-assisted heating and cooling system for a house in Northern of Iran", *Journal of Renewable and Sustainable Energy*, Vol. 9, No. 4, (2017), 045101. (https://doi.org/10.1063/1.5000288).

24. Hoseinzadeh, S., Hadi Zakeri, M., Shirkhani, A. and Chamkha, A.J., "Analysis of energy consumption improvements of a zero-energy building in a humid mountainous area", *Journal of Renewable and Sustainable Energy*, Vol. 11, No. 1, (2019), 015103. (https://doi.org/10.1063/1.5046512).

25. Yousef Nezhad, M.E. and Hoseinzadeh, S., "Mathematical modelling and simulation of a solar water heater for an aviculture unit using MATLAB/SIMULINK", *Journal of Renewable and Sustainable Energy*, Vol. 9, No. 6, (2017), 063702. (https://doi.org/10.1063/1.5010828).

26. REN21, Renewables 2016 global status report, (2016). (https://www.ren21.net/wp-content/uploads/2019/05/REN21_GSR2016_FullReport_en_11.pdf).

27. https://www.irimo.ir.

28. https://earthexplorer.usgs.gov/.

29. https://desktop.arcgis.com/.

30. Kavyani, M.R. and Alijani, B., The foundation of climatology, Tehran: Samt Press, (2005). (In Farsi). (https://samta.samt.ac.ir/content/9117/%D9%85%D8%A8%D8%A7%D 9%86%DB%8C-%D8%A2%D8%A8-%D9%88 %D9%87%D9%88%D8%A7%D8%B4%D9%86%D8%A7%D8%B3% DB%8C).

31. Rich, P.M., Dubayah, R., Hetrick, W.A. and Saving, S.C., "Using viewshed models to calculate intercepted solar radiation: Applications in ecology", *American Society for Photogrammetry and Remote Sensing Technical Papers*, (1994), 524-529. (http://professorpaul.com/publications/rich_et_al_1994_asprs.pdf).

32. Rich, P.M. and Fu, P., "Topoclimatic habitat models", *Proceedings of the Fourth International Conference on Integrating GIS and Environmental Modeling*, (2000). (http://precisionviticulture.com/files/rich_2000_topoclimate_gisem4_96 .pdf).

33. Fu, P., "A geometric solar radiation model with applications in landscape ecology", Ph.D. Thesis, Department of Geography, University of Kansas, Lawrence, Kansas, USA, (2000). (https://biosurvey.ku.edu/geometric-solar-radiation-model-applications-landscape-ecology).

34. Fu, P. and Rich, P.M., "The solar analyst 1.0 manual", Helios Environmental Modeling Institute (HEMI), USA, (2000). (http://professorpaul.com/publications/fu_rich_2000_solaranalyst.pdf).

35. Fu, P. and Rich, P.M., "A geometric solar radiation model with applications in agriculture and forestry", *Computers and Electronics in Agriculture*, Vol. 37, (2002), 25-35. (https://doi.org/10.1016/S0168-1699 (02)00115-1).

36. Bakirci, K., "Correlations for estimation of daily global solar radiation with hours of bright sunshine in Turkey", *Energy*, Vol. 34, No. 4, (2009), 485-501. (https://doi.org/10.1016/j.energy.2009.02.005).

37. Besharat, F., Dehghan, A.A. and Faghih, A.R., "Empirical models for estimating global solar radiation: A review and case study", *Renewable*

and Sustainable Energy Reviews, Vol. 21, (2013), 798-821. (https://doi.org/10.1016/j.rser.2012.12.043).

38. Chen, J.L., Li, G.S., Xiao, B.B., Wen, Z.F., Lv, M.Q., Chen, C.D., Jiang, Y., Wang, X.X. and Wu, S.J., "Assessing the transferability of support vector machine model for estimation of global solar radiation from air temperature", *Energy Conversion and Management*, Vol. 89, (2015), 318-329. (https://doi.org/10.1016/j.enconman.2014.10.004).

39. Zolfaghari, H., Earth's climate, Razi University Press, Kermanshah, (2014). (https://lib.razi.ac.ir/).

40. Alijani, B., Iran's climate,Tehran: Payame Noor University Press, (2012). (https://samta.samt.ac.ir/).

41. Li, D., "Using GIS and remote sensing techniques for solar panel installation site selection", Master's Thesis, University of Waterloo, (2013). (http://hdl.handle.net/10012/7960).